43rd Aerospace Sciences Meeting and Exhibit, January 10–13, 2005, Reno, Nevada

Multi-point Wing Planform Optimization via Control Theory

Kasidit Leoviriyakit*, and Antony Jameson†
Stanford Univerisity, Stanford, CA, 94305-4035, USA

This paper focuses on wing optimization via control theory using a multi-point design method. Based on the design methodology previously developed for wing section and planform optimization at a specific flight condition, it searches for a single wing shape that performs well over a range of flight conditions. A new cost function is defined as the weighted sum of cost functions from a range of important flight conditions. Results of multi-point optimization of a long range transport aircraft show that improvement at each flight condition is not as large as the result from single-point optimization at one of the design points. However improvement in performance measures such as drag divergence Mach number and the lift-to-drag ratio over a range of Mach numbers is significantly greater.

I. Introduction

AERODYNAMIC shape optimization has become a standard practice today. It is widely accepted for optimizing the performance at one specific point. However, an important issue for single-point design is the performance penalty suffered by the same shape at other operating points. One way to seek a good compromise between multiple operating points is through multi-point optimization.

While multi-point design can be extended to most single-point design tools, the ultimate need is the development of an automated multi-point design tool. Here we formulate "automatic shape optimization via control theory" by combining computational fluid dynamics (CFD) with gradient-based optimization techniques, where the gradient is calculated based on the use of the control theory. For a wing design problem, the wing is treated as a device to control the flow to produce lift with minimum drag while satisfying a set of constraints governed by the flow equations and meeting other requirements such as low structural weight, sufficient fuel volume, and acceptable stability. This approach is radically different from conventional optimization methods. It treats the shape as a free surface and drives the flow solution, shape sensitivity, and final shape all to convergence simultaneously. Thus this approach is extremely efficient. During the last decade this method has been extensively developed to improve wing section shapes[1,2,3,4,5] and wing planforms.[6,7,8,9,10,11]

Our previous works[6,7,8,9,10] reported design methodology for wing planform optimization at a cruise condition. The main objective was to reduce drag of the airplane at constant lift, using the wing structural weight as a constraint to prevent un-realistic designs. Wing section and planform shapes were parameterized by mesh points and then used as the design variables. By allowing both section and planform variations, we could reduce both drag and structural weight of the airplane simultaneously while meeting other requirements such as lift, sufficient fuel volume, and stability constraints.

In this work, we report improvements in the wing design, using multi-point design. The optimum shape yields the maximum combined-benefit at multiple flight conditions such as cruise, dive, and other off-design conditions. The objective function is redefined to reflect multiple needs, using a weighted linear combination among several objectives at different flight conditions. Results of multi-point optimization of a long-range transport aircraft show significant improvements in drag divergence Mach number, thus improving the performance of the airplane.

*Doctoral Candidate, Department of Aeronautics and Astronautics, AIAA Member
†Thomas V. Jones Professor of Engineering, Department of Aeronautics and Astronautics, AIAA Member.

II. Mathematical formulation

A. The control theory approach to wing design problems

The control theory approach has been proposed for shape design since 1974[12] but it did not have much impact on aerodynamic design until its application to transonic flow.[1] The major impact arose from its capability to effectively handle a design problem that involves a large number of design variables and is governed by a complex mathematical model, such as fluid flow. The control theory approach is often called the adjoint method since the necessary gradients are obtained through the solution of the adjoint equations of the governing equations.

In the context of control theory, a wing design problem can be considered as:

$$\begin{aligned} Minimizing \quad & I(w,S) \\ w.r.t \quad & S \\ subjected\ to \quad & R(w,S)=0 \end{aligned}$$

where w is the flow variable, S is the vector of wing design parameters, and $R(w,S)=0$ is the flow equation.

For instance, for a drag minimization problem we can take $I = C_D$ which is an integral of flow w (pressure and shear force) over the wing S (represented by parameters such as airfoils and planform). We modify S (the airfoils and planform) to reduce the drag. The pressure and shear force are obtained from the flow equation $R=0$ using CFD.

A change in S results in a change

$$\delta I = \left[\frac{\partial I}{\partial w}\right]^T \delta w + \left[\frac{\partial I}{\partial S}\right]^T \delta S, \tag{1}$$

and δw is determined from the equation

$$\delta R = \left[\frac{\partial R}{\partial w}\right] \delta w + \left[\frac{\partial R}{\partial S}\right] \delta S = 0. \tag{2}$$

The finite difference approach attempts to solve δw from equation (2) and substitute it into equation (1) to calculate δI. For a design problem of n design parameters e.g. $\mathcal{O}(S) = n$, this procedure requires a well-converged solution of $n+1$ flow analysis problems to obtain the design sensitivities. Thus it becomes impractical when n becomes large.

For an adjoint approach, we try to avoid solving for δw. This is done by introducing a Lagrange multiplier ψ, and subtracting the variation δR from the variation δI without changing the result. Thus, equation (1) can be replaced by

$$\begin{aligned} \delta I &= \left[\frac{\partial I}{\partial w}\right]^T \delta w + \left[\frac{\partial I}{\partial S}\right]^T \delta S - \psi^T \left(\left[\frac{\partial R}{\partial w}\right] \delta w + \left[\frac{\partial R}{\partial S}\right] \delta S \right) \\ &= \left\{ \left[\frac{\partial I}{\partial w}\right]^T - \psi^T \left[\frac{\partial R}{\partial w}\right] \right\} \delta w + \left\{ \left[\frac{\partial I}{\partial S}\right]^T - \psi^T \left[\frac{\partial R}{\partial S}\right] \right\} \delta S \end{aligned} \tag{3}$$

Choosing ψ to satisfy the adjoint equation,

$$\left[\frac{\partial R}{\partial w}\right]^T \psi = \left[\frac{\partial I}{\partial w}\right], \tag{4}$$

the first term is eliminated, and we find that

$$\delta I = \mathcal{G}^T \delta S, \tag{5}$$

where

$$\mathcal{G}^T = \left[\frac{\partial I}{\partial S}\right]^T - \psi^T \left[\frac{\partial R}{\partial S}\right].$$

The advantage is that equation (5) is independent of δw, with the result that the gradient of I with respect to an arbitrary number of design variables can be determined without the need for additional flow-field evaluations.

Once the gradient vector $\mathcal{G}$ has been established, it may now be used to determine a direction of improvement. The simplest procedure is to make a step in the negative gradient direction (steepest descent method) by setting

$$\delta S = -\lambda \mathcal{G}$$

where λ is positive and small enough that the first variation is an accurate estimate of δI. The variation of the cost function then becomes

$$\begin{aligned} \delta I &= -\lambda \mathcal{G}^T \mathcal{G} \\ &\leq 0 \end{aligned}$$

More sophisticated search procedures may be used such as quasi-Newton methods, which attempt to estimate the second derivative $\frac{\partial^2 I}{\partial S_i \partial S_j}$ of the cost function from changes in the gradient $\frac{\partial I}{\partial S}$ in successive optimization steps. These methods also generally introduce line searches to find the minimum in the search direction which is defined at each step. Reference[13] provides a good description for those techniques. However, not all the techniques are practical for our wing design problem. Line searches, for example, would require extra flow calculations, which we try to avoid.

B. Design using the Navier-Stokes equations

In this section we illustrate the application of control theory to aerodynamic design problems, using the three-dimensional compressible Navier-Stokes equations as a mathematical model. For convenience, let ξ_1, ξ_2, and ξ_3 denote the transformed coordinates and a repeated index i imply a summation over $i = 1$ to 3. Then, in a fixed computational domain the flow equation $R(w, S) = 0$ takes the form

$$\frac{\partial (Jw)}{\partial t} + \frac{\partial (F_i - F_{vi})}{\partial \xi_i} = 0 \quad \text{in } \mathcal{D}, \tag{6}$$

where J is the cell volume, F_i and F_{vi} are the inviscid and viscous terms which have the form

$$F_i = S_{ij} f_j \quad \text{and} \quad F_{vi} = S_{ij} f_{vj}.$$

Here S_{ij} is the coefficient of the Jacobian matrix of the transformation which represents the projection of the ξ_i cell face along the Cartesian x_j axis. Moreover, because the computational boundary usually aligns with the body surface, S_{ij} on the boundary also represents the geometry we are redesigning.

Suppose we want to minimize the cost function of a boundary integral

$$I = \int_{\mathcal{B}} \mathcal{M}(w, S)\, d\mathcal{B}_\xi \tag{7}$$

where the integral of $\mathcal{M}(w, S)$ could be a pure aerodynamic cost function such drag coefficient, or a multidisciplinary cost function such as combination of drag and structural weight which is shown to be necessary for a planform design problem in references.[6, 7, 8, 9, 10]

In the steady flow the transient term of equation (6) drops out and the the adjoint problem can be formulated by combining the variations of equations (7) and (6) using the Lagrange multiplier ψ as

$$\delta I = \int_{\mathcal{B}} \delta \mathcal{M}(w, S)\, d\mathcal{B}_\xi - \int_{\mathcal{D}} \psi^T \frac{\partial}{\partial \xi_i} \delta (F_i - F_{vi})\, d\mathcal{D}_\xi$$

If ψ is differentiable, the second term on the right hand side can be integrated by parts, resulting

$$\delta I = \int_{\mathcal{B}} \delta \mathcal{M}(w, S)\, d\mathcal{B}_\xi - \int_{\mathcal{B}} n_i \psi^T \delta (F_i - F_{vi})\, d\mathcal{B}_\xi + \int_{\mathcal{D}} \frac{\partial \psi^T}{\partial \xi_i} \delta (F_i - F_{vi})\, d\mathcal{D}_\xi \tag{8}$$

The terms $\delta\mathcal{M}$, δF_i, and δF_{vi} can be split into contributions associated with δw and δS using the subscript I and II to distinguish the variation of the flow solution and those associated with the metric variations as

$$\delta \mathcal{M} = [\mathcal{M}_w]_I\, \delta w + \delta \mathcal{M}_{II}, \quad \delta F_i = [F_{iw}]_I\, \delta w + \delta F_{iII}, \text{ and } \quad \delta F_{vi} = [F_{viw}]_I\, \delta w + \delta F_{viII}.$$

By collecting all the terms that multiply δw of equation (8), the adjoint equation can be formulated. However since the velocity derivatives $\frac{\partial u_i}{\partial x_j}$ in the viscous flux are not explicitly expressed in terms of the state variable w, it is more convenient to introduce the transformation to the primitive variable $\tilde{w}^T = (\rho, u_1, u_2, u_3, p)$, and the relations $\delta w = M\delta\tilde{w}$. This yields the adjoint equations for the Navier-Stokes equation as

$$\left[S_{ij}\frac{\partial f_j}{\partial w}\right]^T \frac{\partial \psi}{\partial \xi_i} - {M^{-1}}^T \tilde{L}\psi = 0 \quad \text{in } \mathcal{D} \tag{9}$$

where

$$\begin{aligned}
(\tilde{L}\psi)_1 &= -\tfrac{p}{\rho^2}\tfrac{\partial}{\partial\xi_l}\left(S_{lj}\kappa\tfrac{\partial\theta}{\partial x_j}\right)\\
(\tilde{L}\psi)_{i+1} &= \tfrac{\partial}{\partial\xi_l}\left\{S_{lj}\left[\mu\left(\tfrac{\partial\phi_i}{\partial x_j}+\tfrac{\partial\phi_j}{\partial x_i}\right)+\lambda\delta_{ij}\tfrac{\partial\phi_k}{\partial x_k}\right]\right\}\\
&+ \tfrac{\partial}{\partial\xi_l}\left\{S_{lj}\left[\mu\left(u_i\tfrac{\partial\theta}{\partial x_j}+u_j\tfrac{\partial\theta}{\partial x_i}\right)+\lambda\delta_{ij}u_k\tfrac{\partial\theta}{\partial x_k}\right]\right\}\\
&- \sigma_{ij}S_{lj}\tfrac{\partial\theta}{\partial\xi_l} \qquad\qquad \text{for} \quad i=1,2,3\\
(\tilde{L}\psi)_5 &= \tfrac{1}{\rho}\tfrac{\partial}{\partial\xi_l}\left(S_{lj}\kappa\tfrac{\partial\theta}{\partial x_j}\right),
\end{aligned}$$

using $\psi_{j+1} = \phi_j$ for $j = 1, 2, 3$ and $\psi_5 = \theta$.

The form of the adjoint boundary conditions depends on the cost function. Table 1 summarizes some of the commonly used cost functions.

Table 1. Adjoint boundary conditions for various cost functions

Category	I	Adjoint boundary conditions
Drag minimization	$C_D = \int_{\mathcal{B}} q_i\tau_i dS$	$\phi_k = q_k$
Weight minimization	$C_W = \frac{-\beta}{cos(\Lambda)^2}\oint_{\mathcal{B}} p(\xi_1,\xi_3)K(\xi_3)S_{22}d\xi_1 d\xi_3$	$\psi_{j+1}n_j = \frac{-\beta}{cos(\Lambda)^2}K\frac{S_{22}}{\lvert S_2\rvert}$
Inverse design	$\frac{1}{2}\int_{\mathcal{B}}(p-p_d)^2\,dS$	$\psi_{j+1}n_j = p - p_d$

The remaining terms from equation (8) then yield a simplified expression for the variation of the cost function which defines the gradient

$$\delta I = \int_{\mathcal{B}} \left\{\delta\mathcal{M}_{II} - n_i\psi^T\left[\delta F_i - \delta F_{vi}\right]_{II}\right\} d\mathcal{B}_\xi + \int_{\mathcal{D}} \left\{\frac{\partial\psi^T}{\partial\xi_i}\left[\delta F_i - \delta F_{vi}\right]_{II}\right\} d\mathcal{D}_\xi.$$

This equation can be further simplified by integrating the last term by parts, resulting in

$$\delta I = \int_{\mathcal{B}} \delta\mathcal{M}_{II}\, d\mathcal{B}_\xi - \int_{\mathcal{D}} \psi^T\frac{\partial}{\partial\xi_i}\delta(F_i - F_{vi})_{II}\, d\mathcal{D}_\xi. \tag{10}$$

This simplification turns out to be crucial for planform gradient calculations.

Once this gradient is evaluated, we can follow the design process outlined in section A to get an optimum shape. In addition, based on the fact that the gradient $\mathcal{G}$ is generally of a lower smoothness class than the shape S, it is important to restore the smoothness.[14] This may be affected by passing to a Sobolev inner product of the form

$$\langle u, v\rangle = \int (uv + \epsilon\frac{\partial u}{\partial\xi}\frac{\partial v}{\partial\xi})\, d\xi$$

This is equivalent to replacing $\mathcal{G}$ by $\bar{\mathcal{G}}$, where in one dimension

$$\bar{\mathcal{G}} - \frac{\partial}{\partial\xi}\epsilon\frac{\partial\bar{\mathcal{G}}}{\partial\xi} = \mathcal{G}, \quad \bar{\mathcal{G}} = \text{zero at end points}$$

and making a shape change $\delta S = -\lambda\bar{\mathcal{G}}$. Then for small positive λ

$$\delta I \;=\; -\lambda\langle\bar{\mathcal{G}}, \bar{\mathcal{G}}\rangle \;\leq\; 0$$

guaranteeing an improvement.

III. Implementation

Since a multi-point design is essentially an extension of a single-point design to perform at multiple design conditions, we first review the design methodology of a single-point design for wing section and planform. Then we describe the techniques to combine multiple results together.

A. Single-point planform optimization

During the last decade, research on section optimization for a fixed wing planform have verified that the adjoint method has been perfected for transonic wing design. The process produces a shock free wing very rapidly.

However for the purpose of drag minimization, shock drag is not the only contribution to drag. Table 2 shows a breakdown of the drag for a typical long-range transport aircraft. Clearly, the major contribution

Table 2. Typical drag breakdown of transport aircraft at cruise condition (1 count = 0.0001)

Item	C_D	Cumulative C_D
Wing pressure	120 counts	120 counts
	(15 shock,105 induced)	
Wing friction	45	165
Fuselage	50	215
Tail	20	235
Nacelles	20	255
Other	15	270
	—	
Total	270	

comes from the induced drag (roughly 45 % of the total drag). It is well known that changes in the wing planform such as span, chord distribution, and taper directly affect the induced drag. Moreover, the sweep and section thickness also affect the shock drag. Thus planform optimization has potential to yield large improvement. However these changes also affect the structural weight of the wing. Therefore it is necessary to take into account both the aerodynamics and structural weight. Then the cost function becomes a combination of aerodynamics and structure weight.

1. *Cost function and design parameters*

Following our previous works,[6,7,8,9,10,11] we redesign both wing section and planform to minimize the cost function

$$I = \alpha_1 C_D + \alpha_2 \frac{1}{2} \int_{\mathcal{B}} (p - p_d)^2 dS + \alpha_3 C_W, \qquad (11)$$

The wing section is modeled by surface mesh points and the wing planform is simply modeled by the design variables shown in figure 1 as root chord (c_1), mid-span chord (c_2), tip chord (c_3), span (b), sweepback(Λ), and wing thickness ratio (t). This choice of design parameters will lead to an optimum wing shape that will not require an extensive structural analysis and can be manufactured effectively. In the industry standard, it may require upto three hundred parameters to completely describe the wing planform. Although we demonstrate our design methodology using the simplified planform, our design method is still applicable to the industry standard because the adjoint method is independent of the number of design variables. Thus our method can be easily extend to cover many parameters without an increase in computational cost.

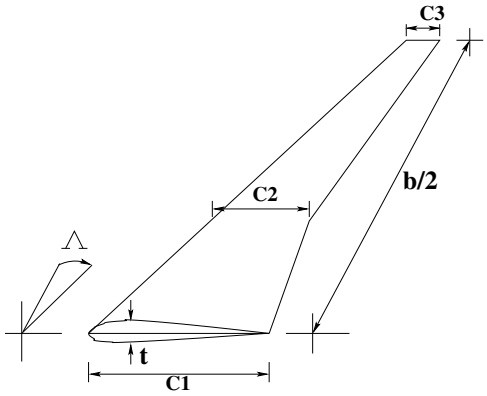

Figure 1. Simplified wing planform of a transport aircraft.

Notice further that this choice of design parameter allows the variation of the wing area. To avoid confusion, all the non-dimensional parameters in the cost function (C_D, C_L, and C_W) are normalized by fixed reference area S_{ref}.

2. *Structural model*

The wing structure is modeled by a box beam shown in figure2, whose major structural material is the box skin. The skin thickness (t_s) varies along the span and resists the bending moment caused by the wing lift. Then, the structural wing weight can be calculated based on material of the skin as

$$W_{wing} = \rho_{mat} g \int_{structual\ span} 2 t_s c_s dl$$

In computation domain, this gives

$$\begin{aligned} C_W &= \frac{W_{wing}}{q_\infty S_{ref}} \\ &= \frac{-\beta}{cos(\Lambda)^2} \oint_{\mathcal{B}} p(\xi_1, \xi_3) K(\xi_3) S_{22} d\xi_1 d\xi_3, \end{aligned} \tag{12}$$

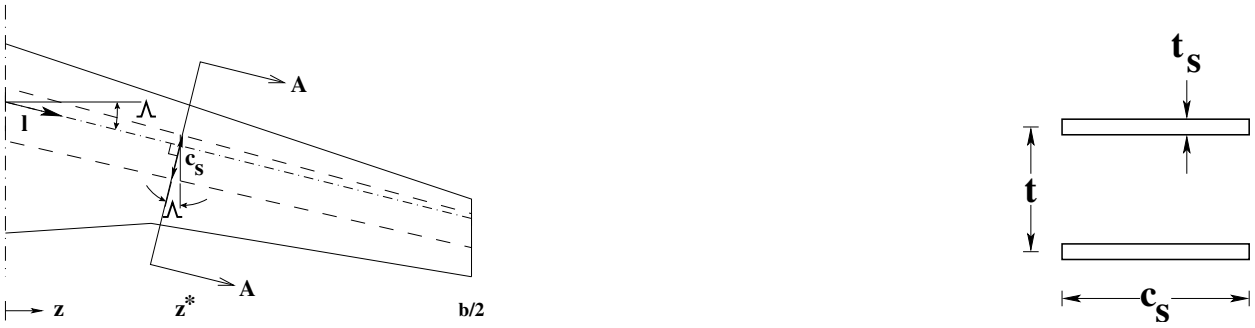

(a) swept wing planform

(b) section A-A

Figure 2. Structural model for a swept wing

Finally to account for the weight of other wing material such as ribs, spars, webs, stiffeners, leading and trailing edges, slats, flaps, main gear doors, primer and sealant, we multiply C_W of equation (12) by a correction factor K_{corr}. This correction factor is based on statistical correlation over a range of aircraft. A good reference is provided by Kroo.[15] Thus

$$C_{W_{tot}} = K_{corr} C_W + K_{corr,0} \tag{13}$$

3. *Choice of the weighting constants*

In equation (11) the coefficient α_2 is introduced to provide the designer some control over the pressure distribution, while the relative importance of drag and weight are represented by the coefficients α_1 and α_3. By varying these constants it is possible to calculate the Pareto front[16] of designs which have the least weight for a given drag coefficient, or the least drag coefficient for a given weight. The relative importance of these constants can be estimated from the Breguet range equation[a];

$$\frac{\delta R}{R} = -\left(\frac{\delta C_D}{C_D} + \frac{1}{log\frac{W_1}{W_2}} \frac{\delta W_2}{W_2} \right)$$

a

$$R = \frac{V}{sfc} \frac{L}{D} log \frac{W_0 + W_f}{W_0}$$

where V is the speed, $\frac{L}{D}$ is the lift-to-drag ratio, sfc is the specific fuel consumption of the engines, W_0 is the landing weight, and W_f is the weight of the fuel burnt.

$$= -\left(\frac{\delta C_D}{C_D} + \frac{1}{log\frac{W_1}{W_2}} \frac{\delta C_W}{\frac{W_2}{q_\infty S_{ref}}}\right).$$

The range of the aircraft is maximized when

$$\frac{\alpha_3}{\alpha_1} = \frac{C_D}{C_{W_2} log\frac{C_{W_1}}{C_{W_2}}}. \tag{14}$$

B. Multi-point planform optimization

Since airplanes operate at many different flight conditions from take-off to landing, it is important to account both design and off-design conditions during the optimization.

Let I_j be the cost function at flight condition j where $j = 1, 2, \ldots, n$ for n flight conditions. Moreover let I_j follow the form defined by equation (11). Then the total cost function becomes

$$I = \beta_1 I_1 + \beta_2 I_2 + \ldots + \beta_n I_n, \tag{15}$$

using

$$\beta_1 + \beta_2 + \ldots + \beta_n = 1$$

Choice of β depends on the importance of the flight condition and may be defined based on the experience of the designer.

Then the gradient can be calculated by weighted average from a different design case as

$$g = \beta_1 g_1 + \beta_2 g_2 + \ldots + \beta_n g_n, \tag{16}$$

and the design process can be expressed as in figure 3.

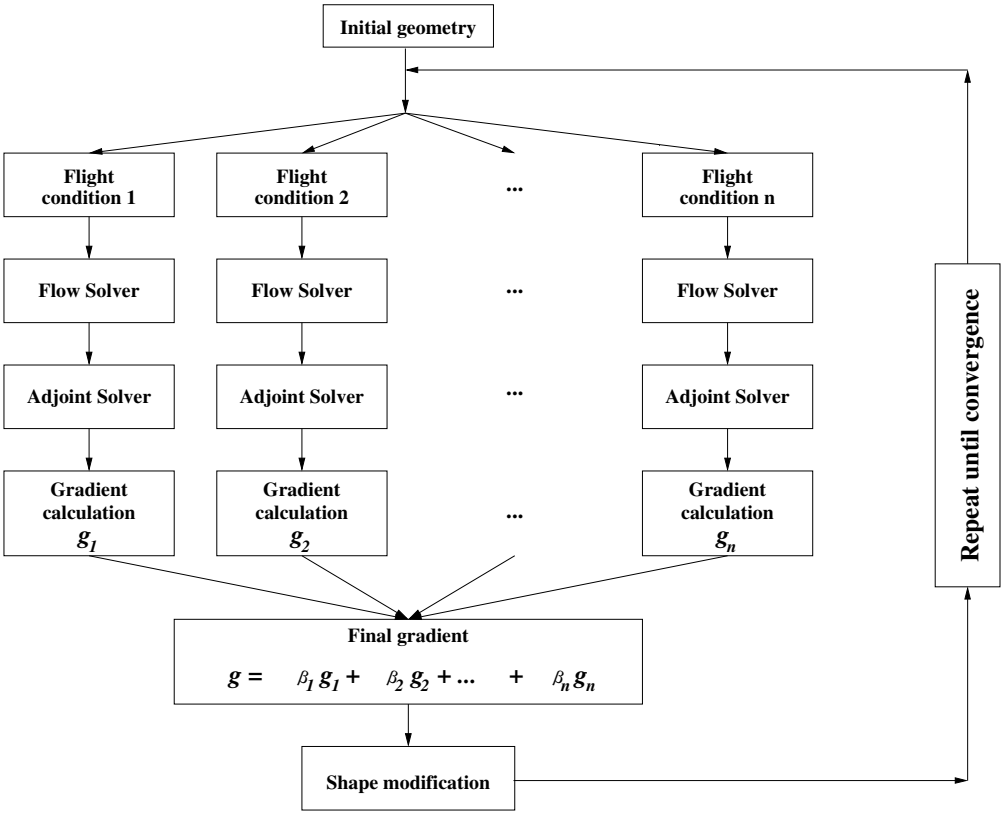

Figure 3. Multi-point design process.

IV. Results

The main goal of any multi-point design is to find a single shape that performs well, over a range of conditions. Because a long range transport aircraft spends most time at the cruise condition, more emphases should be placed on cruise performance.

Our approach in this work is to use multi-point design to relieve undesired characteristics emerging from the cruise-optimized shape at the off-design conditions. From the baseline wing, we start by optimizing wing sections and planform at the cruise condition. Then we check the performance of this wing over a range of Mach number, using C_D as the criterion. As expected, there are some penalties of the same wing at other flight conditions. So we perform multi-point design over this wing. Ultimately, we can redesign both sections and planform to improve the performance. However, it turns out in this work that those penalties can be eliminated by just modifying the wing sections. The results are presented in the following sections.

A. Single-point wing section and planform optimization

Here, we choose the Boeing 747 wing fuselage combination at the cruise condition Mach .85 and a lift coefficient $C_L = 0.45$ as a baseline configuration. The computational mesh is shown in figure 4. On this 256x64x48 grid, the wing sections are represented by 4224 surface mesh points and six planform variables (sweepback, span, chords at three span stations, and wing thickness) are extracted from these mesh points.

We allow simultaneous variations of the sections and planform to optimize the cost function defined in equation (11). We set $\alpha_2 = 0$ and the ratio α_3/α_1 according to equation (14) to maximize the range. After 60 design cycles (total computational cost of flow and gradient calculation is equivalent to 12 flow solutions), improvement in both drag and structural weight can be achieved. Table 3 shows this improvement.

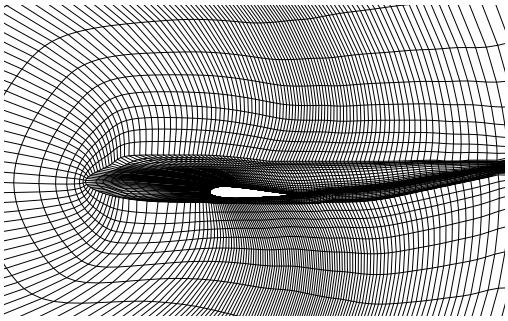

Figure 4. Computational Grid of the B747 Wing Fuselage. Mesh size 256x64x48.

Table 3. Redesign of Boeing 747 at Mach .85 and C_L.45using the Reynolds Averaged Navier-Stokes equations with Baldwin-Lomax turbulent model.

Configuration	C_D (counts)	C_W (counts)
Boeing 747	137	498
Redesign	117	464

Figure 6 shows the changes in the wing planform. The optimum wing has a larger span, a lower sweep angle, and thicker wing sections. The increase in span leads to a reduction in the induced drag, while the section shape changes keep the shock drag low. At the same time the lower sweep angle and thicker wing section reduce the structural weight. Overall, the optimum wing improves both aerodynamic performance and structural weight.

If the Pareto front has a convex shape,[16] by systematically using different ratios of $\frac{\alpha_3}{\alpha_1}$, the Pareto front can be captured. Figure 5 shows this Pareto front. It also shows the point on the Pareto front when $\frac{\alpha_3}{\alpha_1}$ is chosen such that the range of the aircraft is maximized.

To evaluate the performance of this wing, we calculate drag of this wing at fixed C_L.45 at different Mach numbers. Figure 7 shows this drag variation. Although improvement in the drag over a range of Mach number is evident, there is a drag bucket at the design point that should be smoothed out. This can be done using multi-point design as described in the next section.

B. Multi-point redesign of the Boeing 747 wing

The main source of the bucket is the rapid formation of shocks away from the design point, where the flow is essentially shock free. It is well known that according to transonic flow theory[17] a shock-free flow is an

isolated point. Away from this point, shocks will develop. If the shocks are not too strong, we can alleviate this undesired characteristic by just modifying the section alone.

Accordingly we performed a three-point design with the planform fixed at the previously obtained optimum. The flight conditions are indicated in table 4 and the result of this three-point design is shown in figure 8. The variation of drag with Mach number becomes smoother, however at high Mach number, the drag is still too high. So we perform another multi-point design using the condition in table 5. The final variation of drag with Mach number is shown in figure 9. Compared to Boeing 747 drag at the same C_L, improvement in C_D can be seen over the range of Mach number.

Table 4. Flight condition for three-point design

Condition	Mach	Target C_L	β
1	0.84	.45	$\frac{1}{3}$
2	0.86	.45	$\frac{1}{3}$
3	0.90	.45	$\frac{1}{3}$

Table 5. Flight condition for two-point design

Condition	Mach	Target C_L	β
1	0.82	.45	$\frac{1}{2}$
2	0.92	.45	$\frac{1}{2}$

Though we can no longer achieve a shock free solution, the overall design is better as indicated in figures 9 and 10, in which the optimum shape increases the drag divergence Mach number, and improves L/D throughout the range of Mach numbers.

V. Conclusion

The use of multi-point optimization in wing design can yield a substantial improvement over a large range of Mach numbers. The improvement that can be obtained at any one of the design points is not as large as that could be obtained by a single optimization, which usually results in a shock free flow. However, the overall performance, as measured by characteristics such as the drag rise Mach number, is clearly superior.

VI. Acknowledgment

This work has benefited greatly from the support of the Air Force Office of Science Research under grant No. AF F49620-98-1-2005.

References

[1]A. Jameson. Aerodynamic design via control theory. *Journal of Scientific Computing*, 3:233–260, 1988.

[2]A. Jameson. Computational aerodynamics for aircraft design. *Science*, 245:361–371, 1989.

[3]A. Jameson, L. Martinelli, and N. A. Pierce. Optimum aerodynamic design using the Navier-Stokes equations. *Theoretical and Computational Fluid Dynamics*, 10:213–237, 1998.

[4]A. Jameson, J. J. Alonso, J. Reuther, L. Martinelli, and J. C. Vassberg. Aerodynamic shape optimization techniques based on control theory. *AIAA paper 98-2538*, AIAA 29th Fluid Dynamics Conference, Albuquerque, NM, June 1998.

[5]J. R. R. A. Martins. *A Coupled-Adjoint Method for High-Fidelity Aero-Strucural Optimization. PhD Dissertation*, Stanford University, Stanford, CA, October 2002.

[6]K. Leoviriyakit and A. Jameson. Aerodynamic shape optimization of wings including planform variables. *AIAA paper 2003-0210*, 41st Aerospace Sciences Meeting & Exhibit, Reno, Nevada, January 2003.

[7]K. Leoviriyakit, S. Kim, and A. Jameson. Viscous aerodynamic shape optimization of wings including planform variables. *AIAA paper 2003-3498*, 21st Applied Aerodynamics Conference, Orlando, Florida, June 2003.

[8]K. Leoviriyakit and A. Jameson. Aero-structural wing planform optimization. *AIAA paper 2004-0029*, 42nd Aerospace Sciences Meeting & Exhibit, Reno, Nevada, January 2004.

[9]K. Leoviriyakit and A. Jameson. Case studies in aero-structural wing planform and section optimization. *AIAA paper 2004-5372*, 22^{nd} Applied Aerodynamics Conference and Exhibit, Providence, Rhode Island, August 16-19, 2004 2004.

[10]K. Leoviriyakit, S. Kim, and A. Jameson. Aero-structural wing planform optimization using the Navier-Stokes equations. *AIAA paper 2004-4479*, 10th AIAA/ISSMO Multidisciplinary Analysis and Optimization Conference, Albany, New York, August 30 - September 1 2004.

[11]K. Leoviriyakit. *Wing Optimization via an Adjoint Method. PhD Dissertation*, Stanford University, Stanford, CA, December 2004.

[12]O. Pironneau. *Optimal Shape Design for Elliptic Systems*. Springer-Verlag, New York, 1984.

[13]P.E. Gill, W. Murray, and M.H. Weight. *Practical Optimization*. Academic Press, 111 Fifth Avenue, New York, New York 10003, 1981.

[14]A. Jameson and J. C. Vassberg. Studies of alternative numerical optimization methods applied to the brachistochrone problem. *Computational Fluid Dynamics Journal*, 9:281–296, 2000.

[15]Ilan Kroo. Aircraft design: Synthesis and analysis. http://adg.stanford.edu/aa241/AircraftDesign.html, January 2003. Section 10. Structure and weights.

[16]K. Deb. *Multi-Objective Optimization using Evolutionary Algorithms*. John Wiley & Sons, LTD, England, 2002.

[17]C. S. Morawetz. On the non-existence of continuous transonic flows past profiles. *Comm. Pure. Appl. Math.*, 9:45–48, 1956.

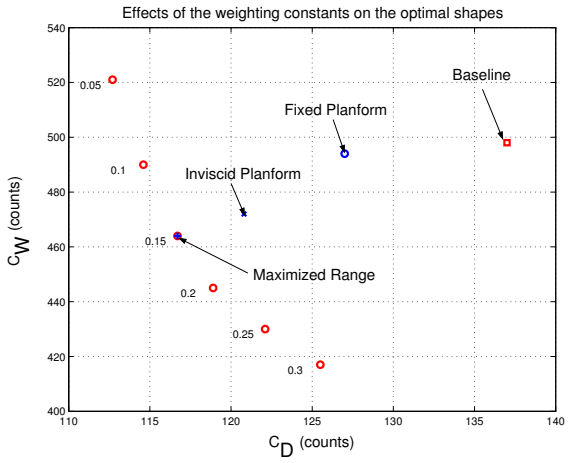

Figure 5. Pareto front of section and planform modifications. The ratios of $\frac{\alpha_3}{\alpha_1}$ are marked for each optimal point.

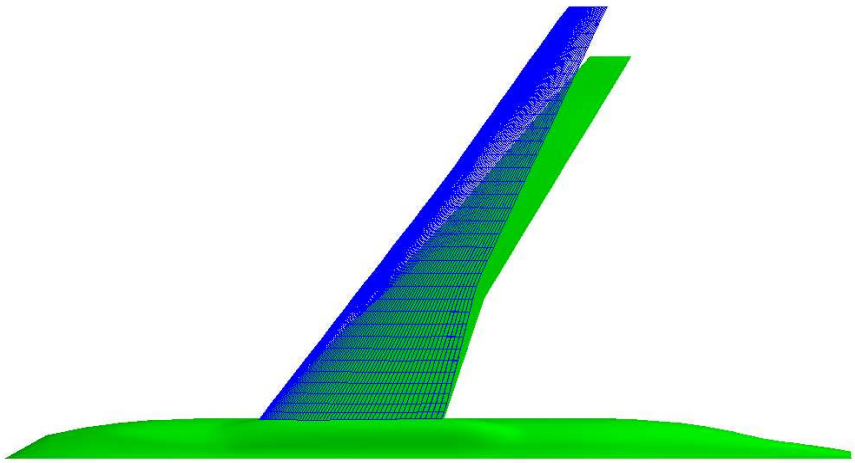

Figure 6. Redesign of Boeing 747 planform using a single-point design method. The baseline (green) and the optimized section-and-planform (blue) geometries of Boeing 747 are over-plotted. The redesigned geometry has a longer span, a lower sweep angle, and thicker wing sections, improving both aerodynamic and structural performances. The optimization is performed at Mach .85 and fixed C_L .45, where $\frac{\alpha_3}{\alpha_1}$ is chosen to maximize the range of the aircraft.

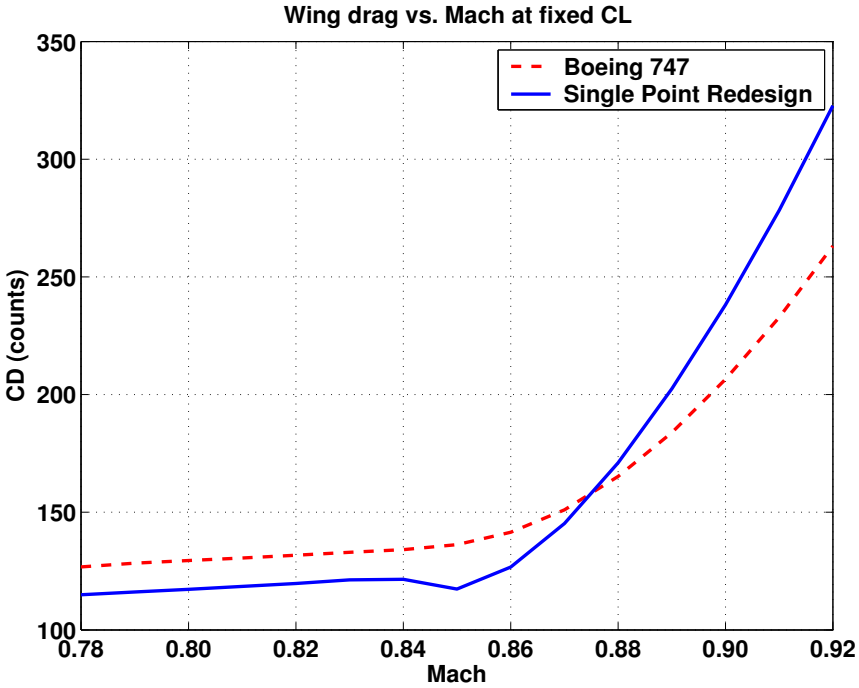

Figure 7. Performance of the single-point-redesigned wing.

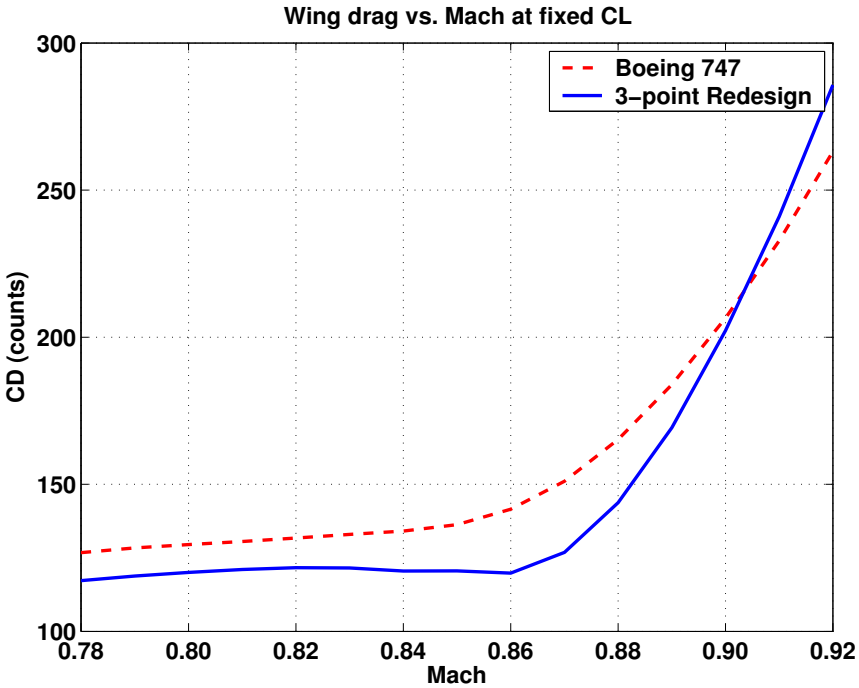

Figure 8. Using three-point design to modify the wing section (planform fixed), the kink of C_D on figure7 can be smoothed out.

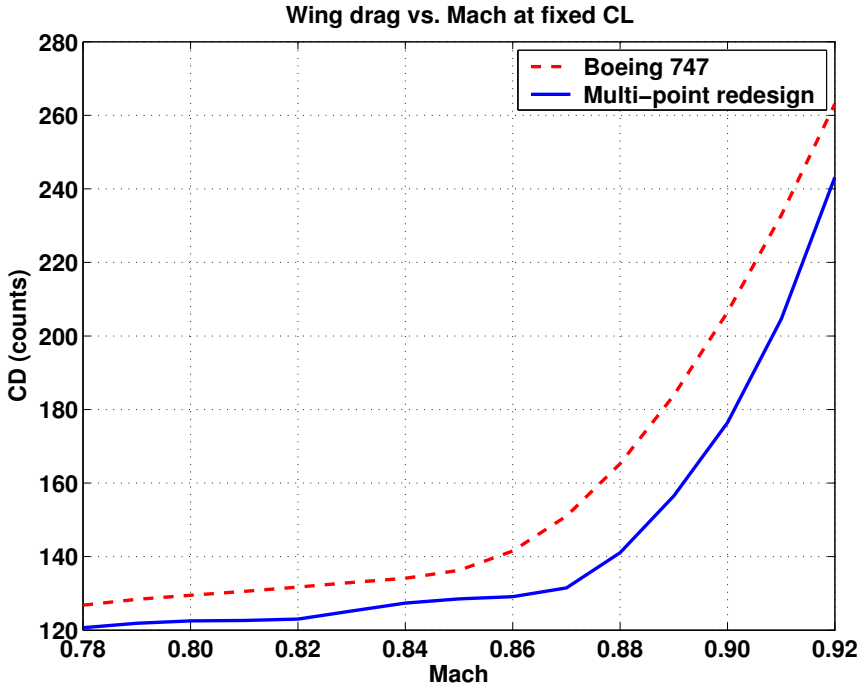

Figure 9. Drag as the function of Mach number at constant lift of the final wing. Two-point design at Mach .82 and .92 is used to modify the wing sections. This plot indicates improvement in the drag divergence Mach number.

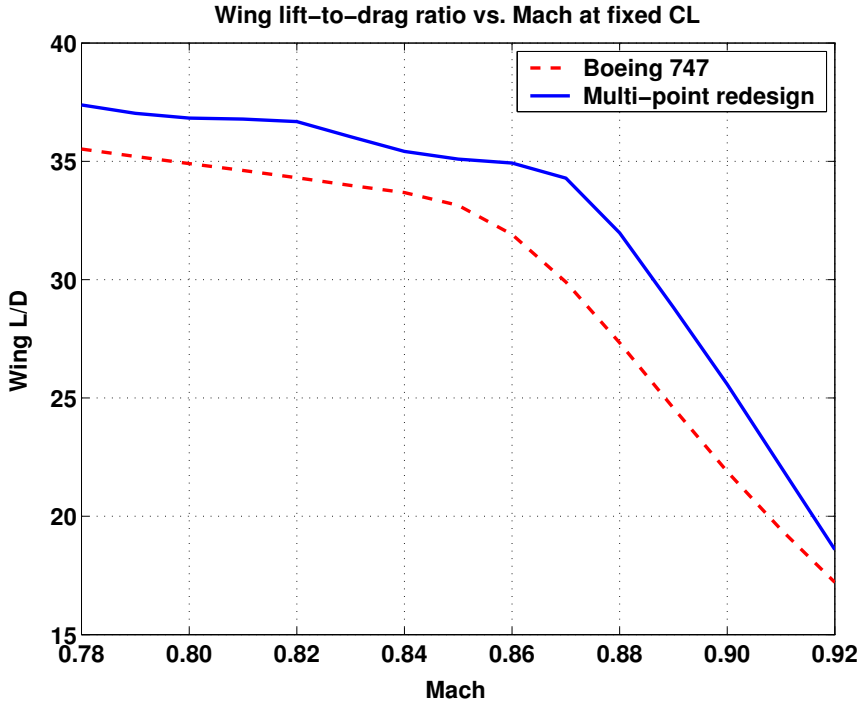

Figure 10. Lift-to-drag as the function of Mach number at constant lift of the final wing. The optimum shape has improvement in $\frac{L}{D}$ over the range of Mach number. To get a smoother variation, further multi-point redesign should be used.